



Three Dimensional Flow Dynamics in Non-linear Duct (90° Elbow) at Predetermined Velocities

Orhorhoro EK¹✉, Ikpe AE², Olorunleke A¹

1. Department of Mechanical Engineering, College of Engineering, Igbiniedion University, Okada, Nigeria

2. Room 142, Department of Mechanical Engineering, University of Benin, Nigeria, P.M.B. 1154

✉ **Corresponding Author:**

Department of Mechanical Engineering, College of Engineering, Igbiniedion University, Okada, Nigeria,

E-mail: ejiroghene.orhorhoro@iuokada.edu.ng, Tel: +2348064699781

Article History

Received: 29 August 2018

Accepted: 27 October 2018

Published: January 2019

Citation

Orhorhoro EK, Ikpe AE, Olorunleke A. Three Dimensional Flow Dynamics in Non-linear Duct (90° Elbow) at Predetermined Velocities. *Indian Journal of Engineering*, 2019, 16, 15-28

Publication License



© The Author(s) 2019. Open Access. This article is licensed under a [Creative Commons Attribution License 4.0 \(CC BY 4.0\)](https://creativecommons.org/licenses/by/4.0/).

General Note



Article is recommended to print as color digital version in recycled paper.

ABSTRACT

Transportation of fluids in the industry especially in the oil and gas sector is a common phenomenon. Thus, analyzing the flow characteristics in elbow ducts is essential for a number of engineering applications, but the limited availability of theories and models to accurately calculate the pressure drop at predetermined velocities is somewhat intricate. Star-CCM+ v5.04 Computational Fluid Dynamics package was used to analyze the pressure characteristics at 5m/s, 10m/s, 20m/s and 40m/s velocity in a non-linear duct (elbow). The results obtained were compared to the calculated ones from the theoretical analysis for the same elbow ducts. It was found that the differences in pressure obtained were mainly as a result of performing the theoretical calculations using one dimensional simplified energy equation while the Computational Fluid Dynamics simulation was performed in two dimensions which

correlate more with what happens in a real flow. The influence of turbulence and boundary layer conditions which was taken into account more accurately by the software also contributed to the errors.

Keywords: Pressure, Duct, CFDs, Velocity, Mass Flow Rate, Simulation, 90° Elbow

1. INTRODUCTION

In the process of transporting fluid from one point to another through ducts or pipes which may either be linear or non-linear depending on the piping system, pressure drop is oftentimes encountered due to resistance to flow. Pressure gain/loss can also be encountered in ducts as a result of change in elevation between the starting and ending point, and may result in minor or major pressure difference (across the duct) which relates to a number of factors such as; pressure gain as a result of fluid head added through pumps, effects of friction acting between the fluid and the wall of the pipe, loss in pressure as a result of the change in elevation of the fluid, friction loss as the fluid flows through bends, pipe fittings etc. [1].

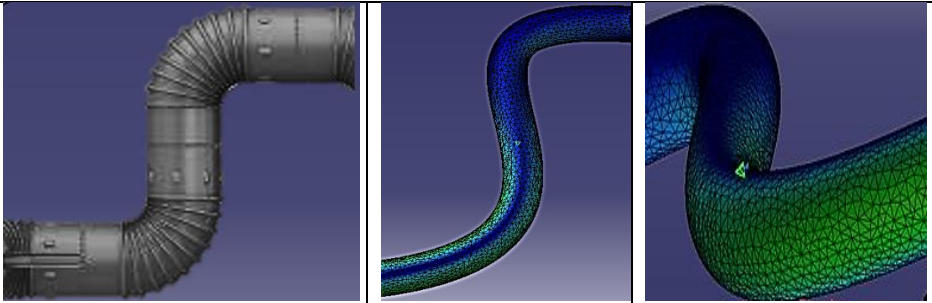
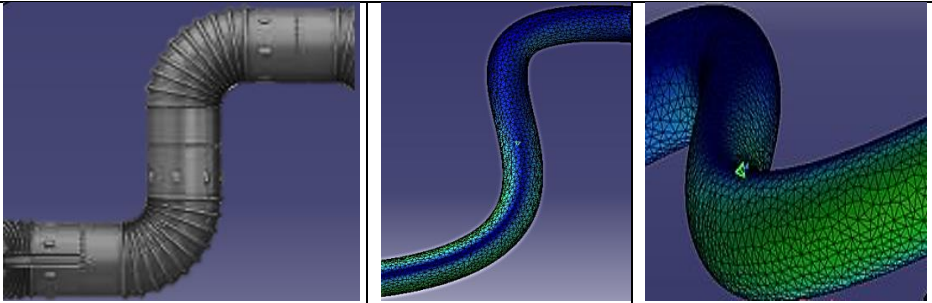
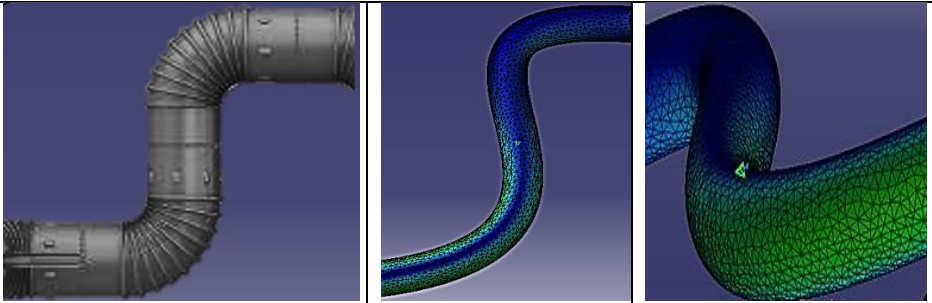
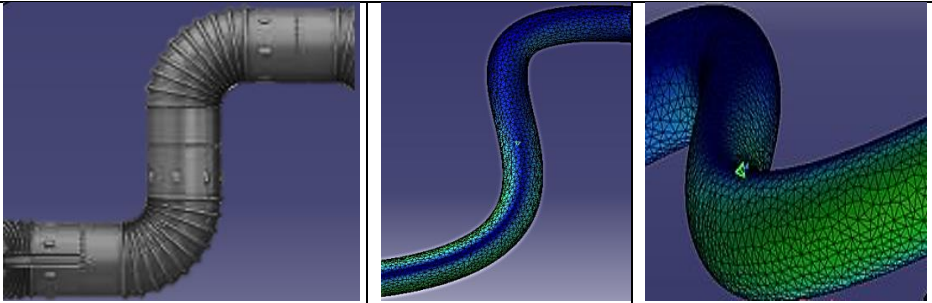
Considering the aforementioned factors, industries such as oil and gas encounter problems in attempt to analyze pressure difference across the piping network. Ellis and Joubert [2] carried out an investigation on turbulent shear flow in curved pipes by comparing the results obtained from two curved rectangular flow to the flow in straight pipe. Crawford *et al.* [3] successfully used frictional effects to predict a single phase pressure drop for turbulent flow at 90° bend, with no available models to separate the flow. Furthermore, Spedding *et al.* [4] in their analysis developed empirical correlations and also determine the pressure drop in elbow bends for single phase laminar and turbulent flow.

Computational Fluid Dynamics (CFDs) is a branch of Fluid Mechanics that applies the principles of numerical analysis and data structures in analyzing pressure distributions in fluid flow [5]. Briley *et al.* [6] in their analyses used Navier-Stokes equation to numerical compute a turbulent flow in 90° square duct channels and pipe bends. The said differential pressure can also be determine by theoretical calculations, the use of gauges etc. but a more specialised tool such as CFDs may also be required when determining the fluid flow at non-linear 90° elbow bends [1, 4, 6,7] which is the primary focus of this study.

2. RESEARCH METHODOLOGY

Mesh convergence studies was carried out for different velocities but at 20m/s velocity, the solution was found to converge at a mesh size of 15mm as shown in Table 1. This mesh size was therefore used to run the analysis for other velocities. Surface mesh was used to mesh the surface of the model. Surface mesh re-triangulates an existing surface in order to improve the overall quality of the surface and optimize it for the volume mesh models. The Trimmer option was selected for the volume meshing. The mesh convergence study is presented in Table 1. The option provides a robust and efficient method of producing a high quality grid for both simple and complex mesh generation problems and produces predominantly hexahedral mesh with minimal cell skewness. Turbulence intensity is a measure of the intensity of turbulence of fluid flow. In flows within a closed conduit, the turbulence intensity varies from 1% to 10% [8].

Table 1 Mesh Convergence study

Mesh Sizes (mm)	Velocity (m/s)			
60	60			
50	50			
40	40			
30	30			
15	20			
10	10			

For the simulation, turbulence intensity was set at 10%. Turbulent length scale is a physical quantity describing the size of the large energy-containing eddies in a turbulent flow. In pipe flows, turbulent length scale can be estimated from the hydraulic diameter and has been shown to vary between 3.8% and 7%. For this simulation, the turbulent length scale was taken as 7% of hydraulic diameter. In the same manner, 5% turbulent velocity scale of the free stream velocity was used in the simulation. In this

study, theoretical calculation and star CCM simulation was used to determine the static and total pressure in non-linear flow system for 5m/s, 10m/s, 20m/s and 40m/s velocities and both the theoretical calculations and simulated results were compared for possible errors and difference. Mesh convergence study for the elbow pipe is presented in Table 1. The channel length of the pipe was 2.6m with pipe diameter of 16.8mm. Mesh control was applied to the model in order to establish some salient factors such as the element shape, mid-side node placement and element size. Curvature based mesh was also applied in order to refine all regions of higher curvature, as these regions are prone to stress formations due to the non-linear shape of the duct. These information are basically for the model development process, and can affect the accuracy of the model and subsequent analysis.

2.1. Boundary Conditions

Table 2 shows the boundary conditions obtained after the analysis for the respective velocities.

Table 2 Boundary conditions

Inlet Velocity (m/s)	Mach number	Boundary Layer Thickness	Mass Flow rate(Inlet) (kg/s)	Turbulence intensity
5	0.0128	0.06670	2.9	0.29881
10	0.0186	0.06041	2.9	0.29881
20	0.0312	0.05471	2.9	0.29881
40	0.121	0.04955	2.9	0.29881

This represents the total pressure (contour), Velocity (vector) and Static Pressure (Contours) for 5m/s, 10m/s, 20m/s and 40m/s velocity at corresponding mass flow rate of 2.9kg/s, 3.6kg/s, 5.4kg/s and 7.8 kg/s respectively. Flow output across the internal gradient of the 90° elbow duct for each velocity is presented in Figure 1 to 12. The turbulent length scale was 6% of the hydraulic diameter while turbulent velocity scale was 8% of the free steam velocity.

2.2. Total Pressure (Contours)



Figure 1 Plot of total pressure at 5m/s

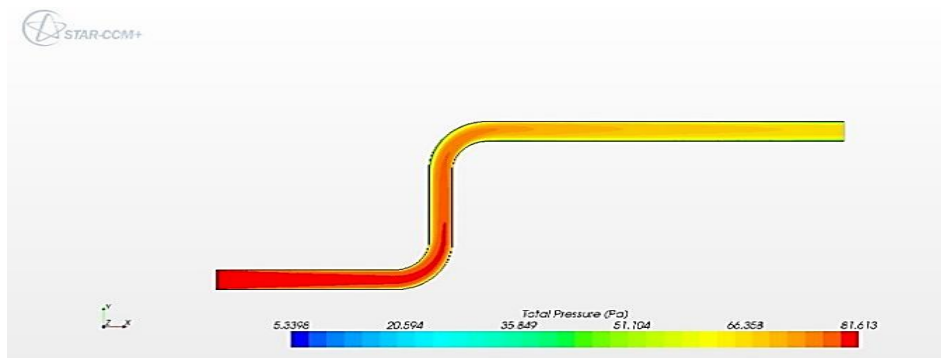


Figure 2 Plot of total pressure at 10m/s

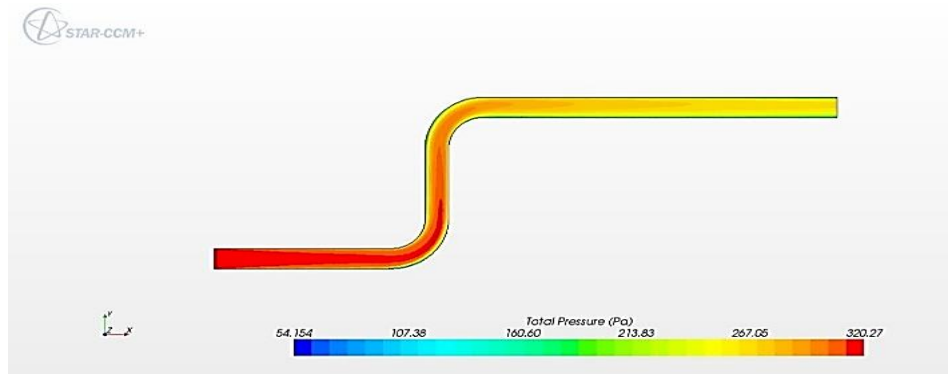


Figure 3 Plot of total pressure at 20m/s

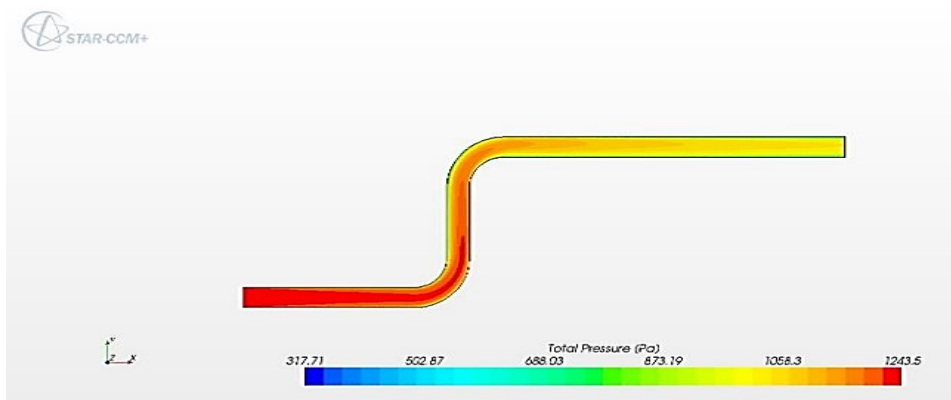


Figure 4 Plot of total pressure at 40m/s

2.3. Velocity (Vector)

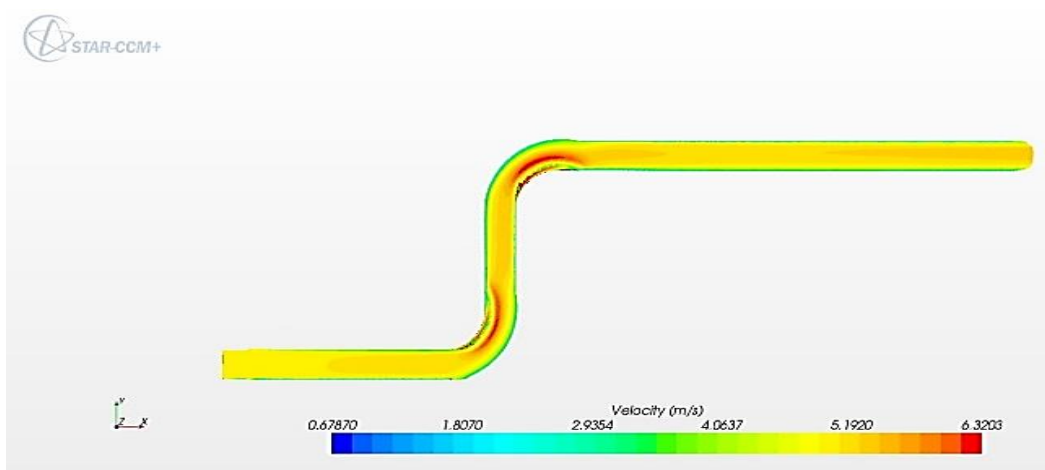


Figure 5 Plot of Velocity at 5m/s

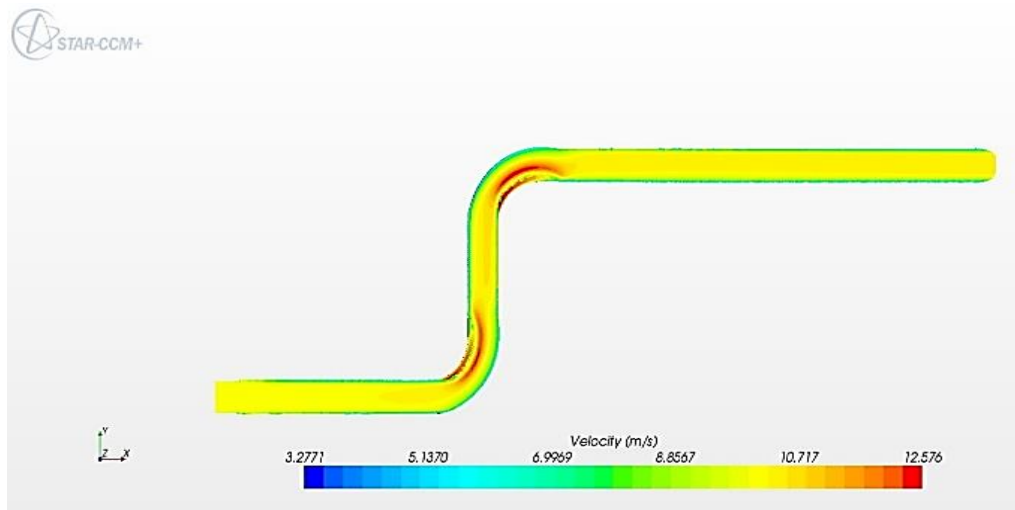


Figure 6 Plot of Velocity at 10m/s

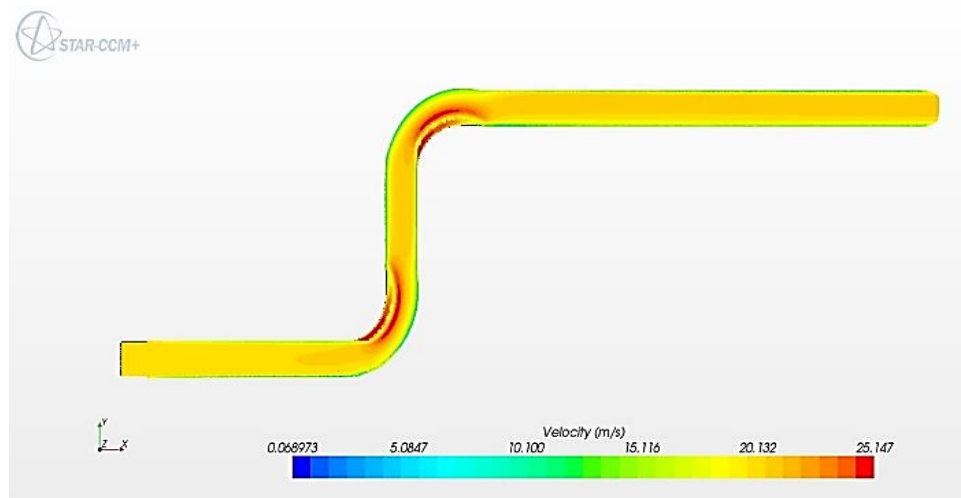


Figure 7 Plot of Velocity at 20m/s

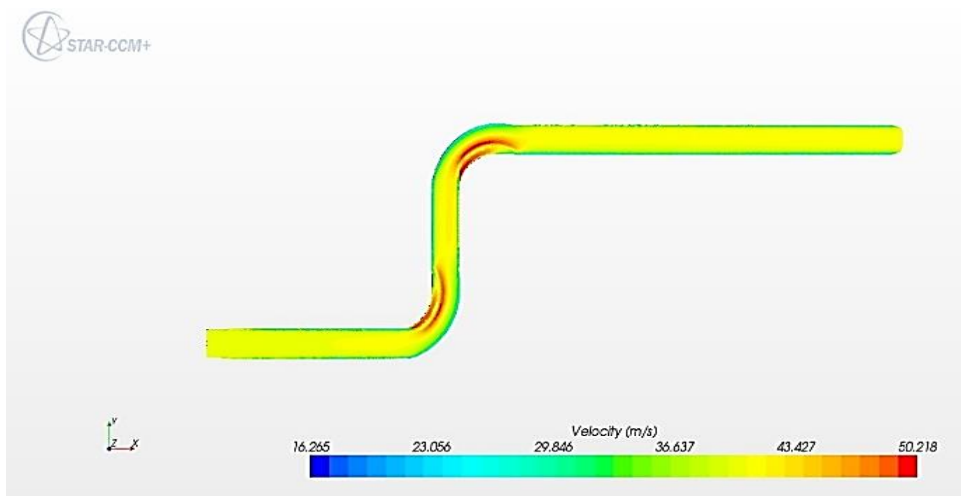


Figure 8 Plot of Velocity at 40m/s

2.4. Static Pressure (Contours)

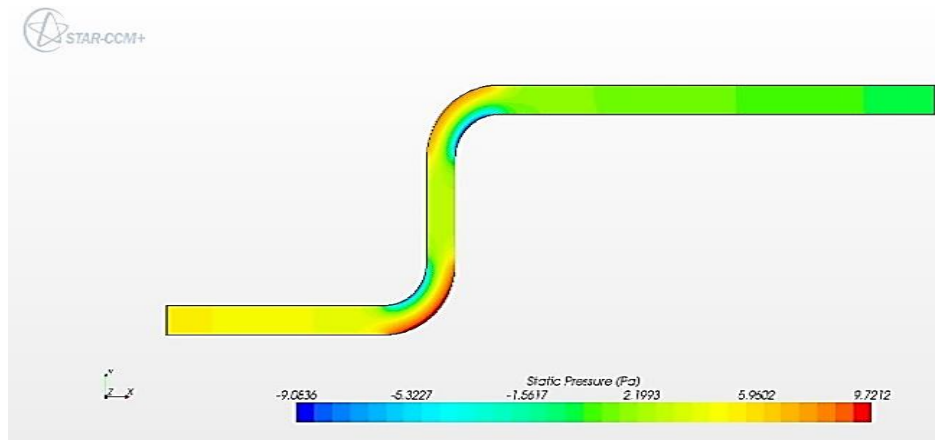


Figure 9 Plot of static pressure at 5m/s

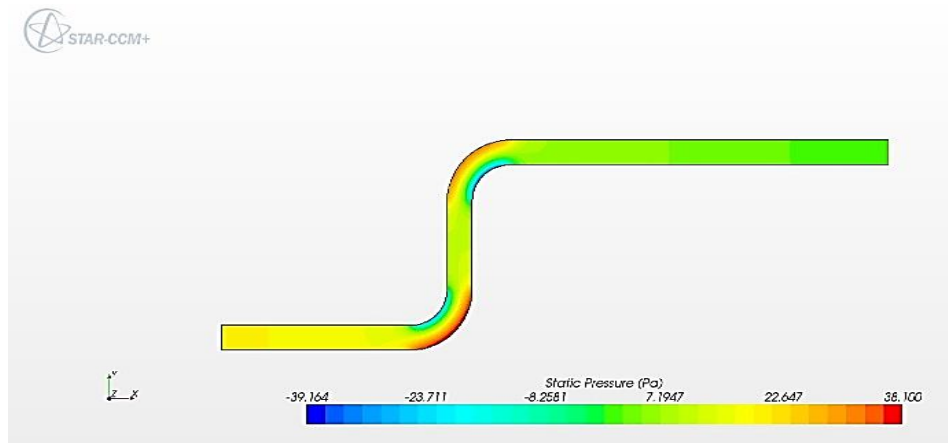


Figure 10 Plot of static pressure at 10m/s

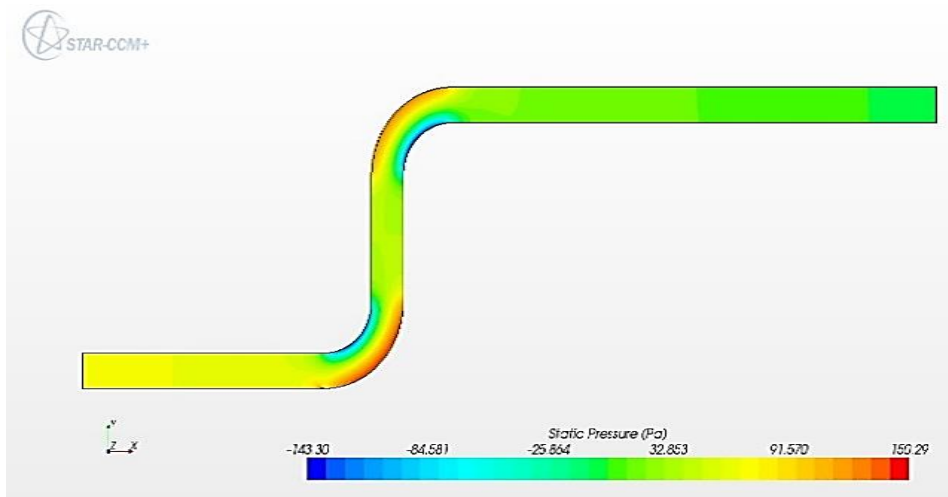


Figure 11 Plot of static pressure at 20m/s

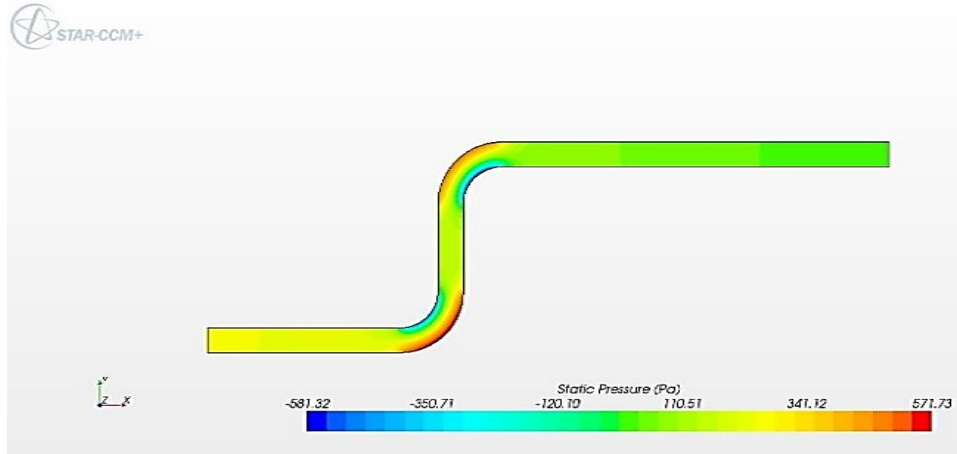


Figure 12 Plot of static pressure at 40m/s

2.5. Theoretical Analysis

Analyzing the flow characteristics in air ducts is essential for a number of engineering applications, but the limited availability of theories and models to accurately determine the pressure condition at predetermined velocities is somewhat intricate. This section involves the application of existing equations in calculating pressure conditions in the elbow duct at different scenarios.

2.6. Calculation of Static Pressure

To find the inlet static pressure by theoretical calculation, Equation (1) was used;

$$P_o = P_{(\text{inlet static})} + 0.5(\rho V^2) \quad (1)$$

where,

P_o = Total inlet pressure (Pa),

$P_{(\text{inlet static})}$ = Inlet static pressure (Pa),

ρ = Density of air (kg/m^3), V = Inlet velocity (m/s).

$$\text{Total Inlet pressure} = \text{Inlet static pressure} + \text{Inlet dynamic pressure} \quad (2)$$

Hence;

$$P_{(\text{Inlet static})} = P_o - 0.5 (\rho V^2) \quad (3)$$

Substituting the values obtained by theoretical calculations for total inlet pressure into Equation (1), the following values were obtained as shown in Table 3;

Table 3 Values Obtained from Theoretical Calculations

Inlet Velocity (V) (m/s)	Density (ρ) (kg/m^3)	The total inlet pressure (P_o) (Pa)	Inlet static pressure $P_{(\text{inlet static})}$ (Pa)
5	1.2	56.900	41.9
10	1.2	118.350	58.35
20	1.2	356.724	116.728
40	1.2	1285.956	325.956

2.7. Pressure loss obtained from 1D Formula

The Energy equation is given by Equation (4)

$$\frac{P_1}{\rho g} + \frac{V_1^2}{2g} + Z_1 - h_{loss} = \frac{P_2}{\rho g} + \frac{V_2^2}{2g} + Z_2 \quad (4)$$

where,

P_1 = The total pressure at the inlet,

P_2 = The total pressure at the outlet which is equal the atmospheric pressure,

V_1 = the inlet velocity, V_2 = the outlet velocity,

Z_1 = the distance between inlet and the datum point,

Z_2 = the distance between outlet and the datum point,

ρ = the density of air at 20°C

For continuity,

$$Q_1 = Q_2 \quad (5)$$

where,

Q_1 = mass flow rate at the inlet,

Q_2 = mass flow rate at the outlet;

Hence, the mass flow rate at the inlet is given by;

$$\rho A_1 V_1 = \rho A_2 V_2 \quad (6)$$

When the inlet and outlet area are the same, and the density are the same, then the inlet velocity is equal to the outlet velocity as shown in Equation (7);

$$V_1 = V_2 \quad (7)$$

Moreover, the outlet pressure is equal to the atmospheric pressure, which is equal zero as shown in Equation (8);

$$P_2 = 0 \quad (8)$$

By substitute the equation 7 and 8 into equation 4, Equation (9) was obtained as follow;

$$\frac{P_1}{\rho g} = (Z_2 - Z_1) + h_{loss} - \frac{P_2}{\rho g} + \frac{(V_2 - V_1)^2}{2g} \quad (9)$$

$$\frac{P_1}{\rho g} = (Z_2 - Z_1) + h_{loss(total)} \quad (10)$$

$$P_1 = \rho g \times [(Z_2 - Z_1) + h_{loss(total)}] \quad (11)$$

2.8. Pressure Losses at the Duct

Three losses happen in the duct as the flow passed from inlet to outlet; these losses are major loss in horizontal length and vertical length, and minor loss in two bends. The following steps were adopted in the pressure loss theoretical calculations for 5m/s velocity.

$$h_{l(total)} = h_{l(\text{major loss x-direction})} + h_{l(\text{major loss x-direction})} + h_{l(\text{minor loss at bend})} \quad (12)$$

$$Re = \frac{\rho V D}{\mu} = \frac{1.2 \times 5 \times 0.4}{1.8 \times 10^{-5}} \quad (13)$$

$$Re = 133,333.33 = 1.33 \times 10^5$$

The flow is turbulent since Re is greater than 4,000. The following represents the theoretical background of the pressure analysis. Major losses due to the horizontal length of the pipe. The head loss due to friction can be obtained;

$$\text{Head loss}_{(\text{major loss x-direction})} = f_{(Re)} \times \frac{L_1}{D} \times \frac{V^2}{2g} \quad (14)$$

Major losses due to the vertical length of the pipe. The head loss due to friction is shown in Equation (15).

$$\text{Head loss}_{(\text{major loss Y-direction})} = f_{(Re)} \times \frac{L_2}{D} \times \frac{V^2}{2g} \quad (15)$$

Minor losses due to the bends of the pipe. The head loss due to friction was obtained as follow:

$$\text{Head loss}_{(\text{minor loss at bend})} = K_l \times \frac{V^2}{2g} \quad (16)$$

Since there is two bends at 90° of the system

$$\text{Head loss}_{(\text{minor loss at bend})} = 2 \times K_l \times \frac{V^2}{2g} \quad (17)$$

The mass flow rate was given by Equation 18;

$$Q = \rho AV \quad (18)$$

where,

Q = The mass flow rate (m³/s),

A = The area for 1m width and 0.4 thick (m²),

V = The velocity (m/s),

ρ = The density of air (kg/m³).

0.4m was used as the area of the duct since the simulation was done in 2D. The following steps were used in the pressure loss; theoretical calculations for 10m/s, 20m/s and 40m/s velocity. Turbulence kinetic energy for Standard k-epsilon turbulence model is given by Equation 19, while turbulent dissipation for Standard k-epsilon turbulence model is given by Equation 20;

$$\frac{\partial}{\partial t}(\rho k) + \frac{\partial}{\partial x_j} \left[\rho u_j k - \left(\mu + \frac{\mu_t}{\sigma_k} \right) \frac{\partial k}{\partial x_j} \right] = \mu_t \left(S_{ij} \frac{\partial u_i}{\partial x_j} - \frac{g_i}{\sigma_{h,t}} \frac{1}{\rho} \frac{\partial \rho}{\partial x_i} \right) - \rho \epsilon - \frac{2}{3} \left(\mu_t \frac{\partial u_i}{\partial x_i} + \rho k \right) \frac{\partial u_i}{\partial x_i} \quad (19)$$

$$\frac{\partial}{\partial t}(\rho \epsilon) + \frac{\partial}{\partial x_j} \left[\rho u_j \epsilon - \left(\mu + \frac{\mu_t}{\sigma_\epsilon} \right) \frac{\partial \epsilon}{\partial x_j} \right] =$$

$$C_{e1} \frac{\epsilon}{k} \left[\mu_t S_{ij} \frac{\partial u_i}{\partial x_j} - \frac{2}{3} \left(\mu_t \frac{\partial u_i}{\partial x_i} + \rho k \right) \frac{\partial u_i}{\partial x_i} \right] - C_{e2} \rho \frac{\epsilon^2}{k} - C_{e3} \rho \frac{\epsilon}{k} \mu_t \frac{g_i}{\sigma_{h,t}} \frac{1}{\rho} \frac{\partial \rho}{\partial x_i} + C_{e4} \rho \epsilon \frac{\partial u_i}{\partial x_i} \quad (20)$$

ρ , k , ϵ , u , σ , S_{ij} represents density, turbulent kinetic energy, turbulent dissipation rate, absolute velocity, turbulence Prandtl number and average tension rate, while C_{e1} , C_{e2} , C_{e3} , C_{e4} standard k-epsilon Turbulence Coefficients.

3. RESULTS AND DISCUSSION

The following results shown in Table 4-9 were obtained from both the theoretical calculations and simulation of flow conditions in the 90° elbow duct, whereas, Figure 13-16 shows the graphical representation for various calculations.

Table 4 Results Obtained from Theoretical Calculations

S/N	Velocity (m/s)	Reynolds number	$f_{(Re)}$	h_l (major loss x-direction) (m)	h_l (major loss Y-direction) (m)
1	5	133,333.33	0.01688	0.4840	0.0753
2	10	266,666.67	0.01477	1.6933	0.2634
3	20	533,333.33	0.01305	5.9845	0.9309
4	40	1,066,666.67	0.01164	21.3656	3.3235

Table 5 Total Inlet Pressure and Mass Flow Rate from Theoretical Calculations

S/N	Velocity (m/s)	h_l (minor loss at bend) (m)	$h_{l \text{ (total)}}$ (m)	$Z_2 - Z_1$ (m)	Total Inlet pressure (Pa)	Mass flow rate (kg/s)
1	5	1.2742	1.8335	3	56.900	2.4
2	10	5.0968	7.0535	3	118.350	4.8
3	20	20.3874	27.3028	3	356.724	9.6
4	40	81.5494	106.2385	3	1285.956	19.2

Table 6 Data from the CFDs Simulation

Inlet Velocity (m/s)	Outlet Velocity (m/s)	Inlet Pressure (pa)	Outlet Pressure (pa)	Inlet mass Flow rate (kg/s)	Outlet mass Flow rate (kg/s)
5	5.328105	5.94	0	2.4	2.4
10	10.54154	21.91	0	4.8	4.8
20	20.97109	81.58	0	9.6	9.6
40	41.65581	285.66	0	19.2	19.2

Table 7 Values Obtained from the CFDs Simulation

Inlet Velocity (m/s)	Inlet total pressure (pa)	Outlet total pressure (pa)	Inlet static pressure (pa)	Outlet static pressure (pa)
5	20.94	17.03	5.94	0
10	81.92	66.67	21.91	0
20	321.58	263.87	81.58	0
40	1245.66	1041.12	285.66	0

Table 8 Total Inlet Pressure (Theoretical Calculation) and Inlet Pressure (Simulation)

Velocity (m/s)	Total Inlet pressure (Pa) theoretical calculation	Total Inlet pressure (Pa) Simulation	% Error Between theoretical calculation and Simulation
5	56.90	20.94	63.20
10	118.35	81.91	30.79
20	356.72	321.58	9.85
40	1285.96	1245.66	3.13

Table 9 Comparing both Total Inlet Pressure for Theoretical Calculation and Simulation

Inlet Velocity (V) (m/s)	Static Inlet pressure from theoretical calculation	Static Inlet pressure from simulation	Percentage of Error
5	41.9	5.94	85.82
10	58.35	21.91	62.45
20	116.728	81.58	30.11
40	325.956	285.66	12.36

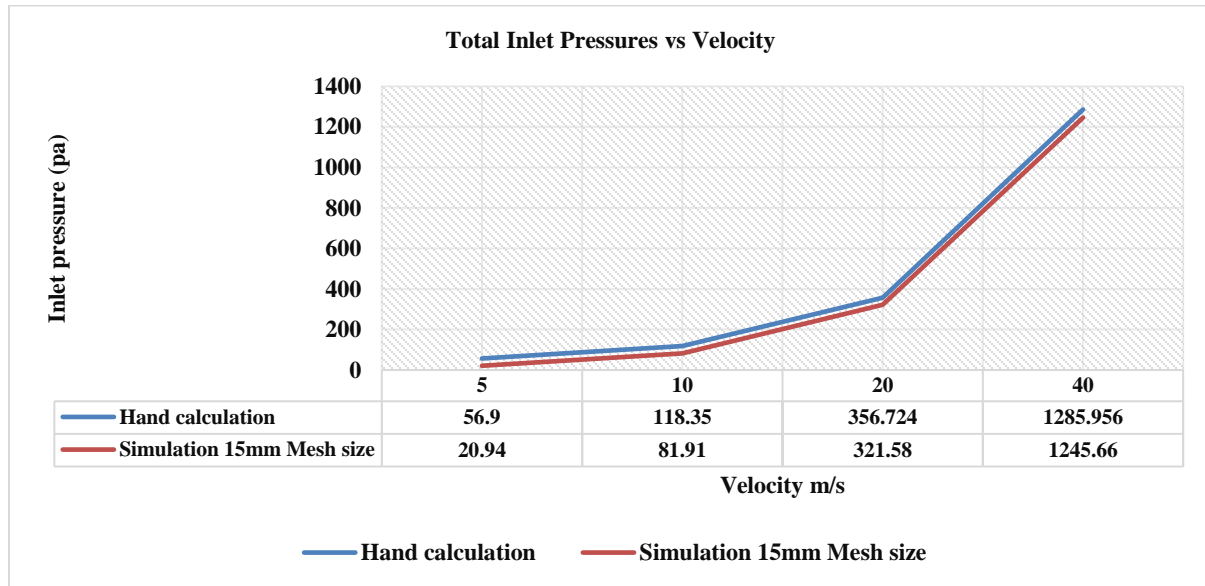


Figure 13 Total Inlet pressure (Theoretical Calculations and Simulation) versus Velocity

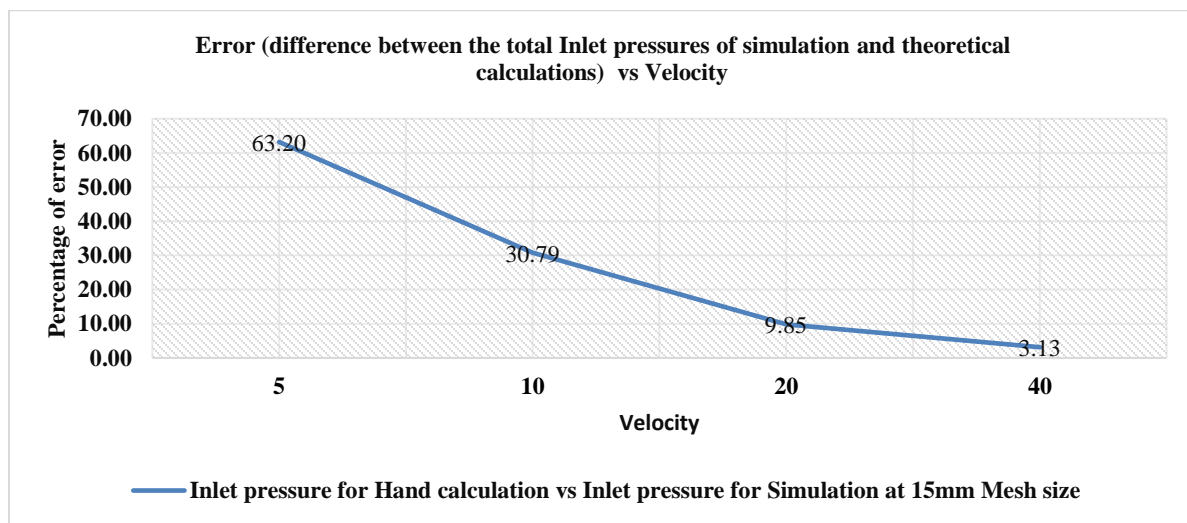


Figure 14 Difference in Total Inlet pressure (Theoretical Calculation and Simulation) versus Velocity

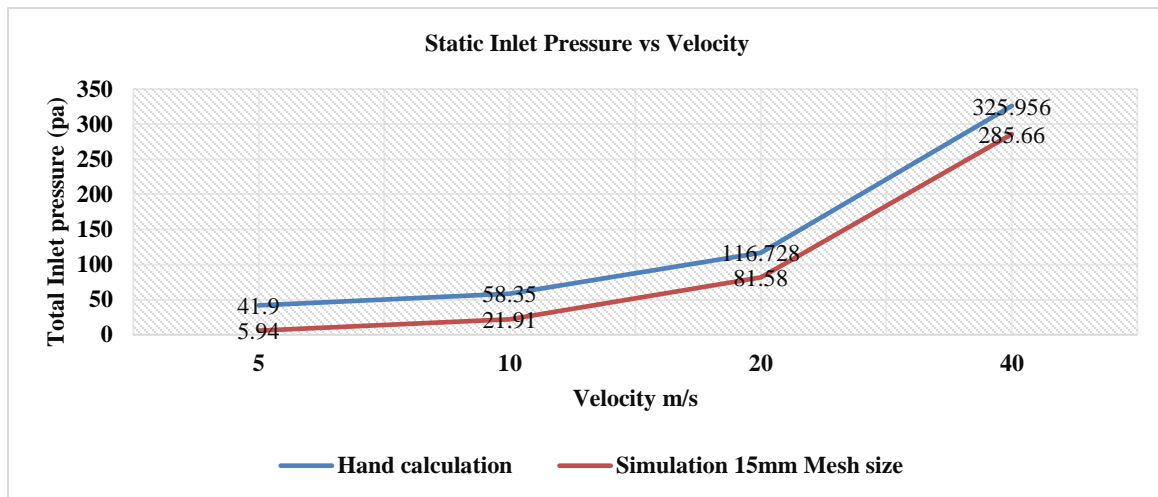


Figure 15 Static Inlet Pressure (Theoretical Calculation and Simulation) versus Velocity

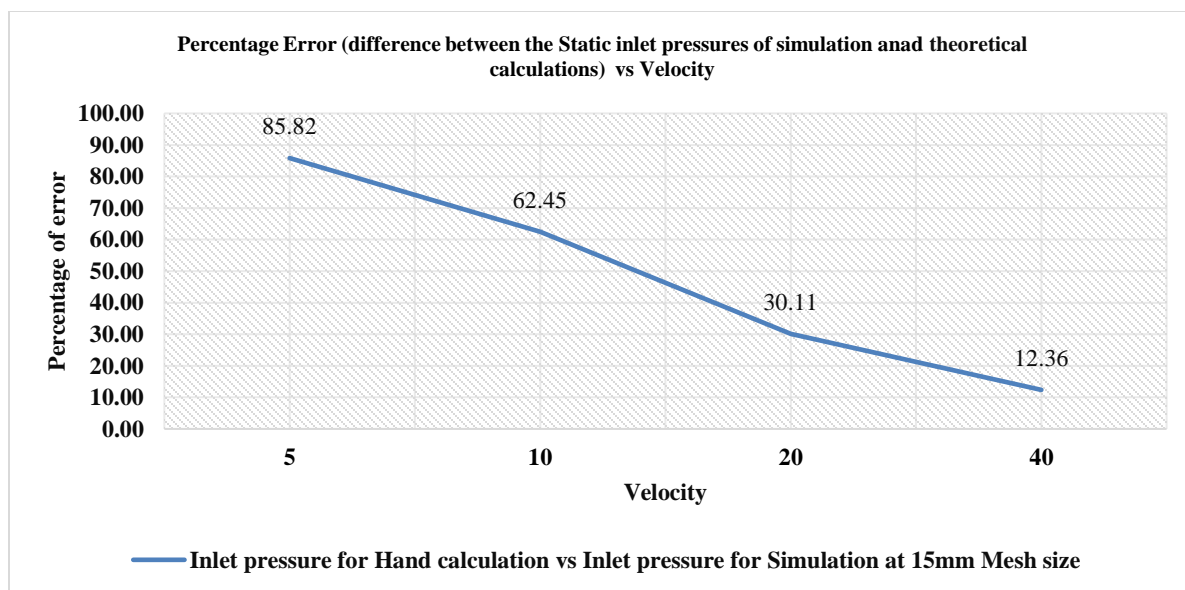


Figure 16 Difference between the Static Inlet Pressures versus Velocity

Figure 13 shows total pressure against inlet velocity for the results of theoretical calculations and simulations, while Figure 14 shows the plot of error between the total inlet pressures and the inlet velocities. Figure 15 depicts the results of plot of static inlet pressures for simulations and theoretical calculations against inlet velocity while Figure 16 shows the plot of error between the static pressures and inlet velocity. As shown in Figure 13 and 15, it can be observed that the pressure increased with increase in velocity. The increase is exponential because the velocity term in the pressure equation is squared. As shown in Figure 14 and 16, it can be observed that the error decreases as velocity is increased from 5m/s to 40m/s. The difference between the results obtained from theoretical calculations and that obtained from CFDs analysis can be explained to be as a result of performing the theoretical calculations in one dimension while the simulation was done in two dimensions.

The one dimension analysis simplifies flows assuming velocity and fluid energy to be the same throughout the flow. The two dimensions is closer and more accurate representation of what is happening in reality where the fluid velocity varies from point to point. Also the effect of other flow parameters such as the boundary layers were not taken into account in one dimension calculation, while its effect was taken into account in the computational fluid dynamics analysis. In general, for simple geometries such as the one used in this analysis, the one dimension pressure loss formula can be used to get a general idea about flow conditions while more detailed analysis can be done in two dimensions or three dimensions for more accurate and detailed results.

Analysis in computational fluid dynamics is affected by the number of grid points (cells) generated to solve the computation. The number of cell generated is a function of the mesh size.

Generally, as the number of cell increases, the results obtained become more accurate while the computational time increases also. However, as the mesh size is made finer and the number of cells increased, a point is reached when the results obtained is not or is marginally affected by the mesh size. At this point, the mesh is said to have converged. The results obtained at this point are usually taken as the solution of the computation. Due to the length of time required to obtain solutions using fine mesh sizes, initial analyses were done using coarse mesh. The mesh size was gradually refined until convergence was achieved. Another important parameter which affected the results obtained from the simulation is the number of iteration to convergence. The iteration steps were increased until the results obtained were stabilized (i.e., the results were no longer changing with time). In general, flow in a two dimensional plane is considered as a special case of a three dimensional if the geometry is symmetrical in one coordinate [9]. However, experiments have shown that two dimensional models give a very close approximation to three dimensional models for symmetrical model [10, 11].

4. CONCLUSION

Three dimensional flow dynamics in non-linear duct (90° elbow) at predetermined velocities were analyzed using Star CCM+, and the flow parameters and characteristics were successfully determined. The results obtained from the simulations were compared with the ones obtained from theoretical calculations. The error between the two results were explained to be as a result of performing the theoretical calculations using one dimensional energy equation, whereas, the simulations were carried out in two dimensions which was a better representation of what happens in real life situation. The effects of boundary layer conditions which was taken into account in the simulations was also a contributing factor to the errors obtained.

Acknowledgement

The authors of this manuscript would like to express their gratitude to Coventry University for providing the support and tools used in achieving the objectives of this paper.

Funding: This research received no external funding.

Conflicts of Interest: The authors declare no conflict of interest.

Nomenclature

CFDs	Computational Fluid Dynamics
P_o	Total inlet pressure
P	Pressure
ρ	Density
V	Velocity
Z_1	Distance between inlet and the datum point
Z_2	Distance between outlet and the datum point
Q	Mass flow rate
A	Area
Kg/s	Kilogram per seconds
m/s	Meters per seconds
Re	Reynold number
K_f	Frictional Factor
K	Turbulent kinetic energy
ϵ	Turbulent dissipation rate
u	Absolute velocity
σ	Turbulence Prandtl number
S_{ij}	Average tension rate
h_l	Head loss

REFERENCE

1. Walker, I. S., Wray, C. P., Dickerhoff, D. J., Sherman, M. H. (2001). Evaluation of Flow Hood Measurements for Residential Register Flows. LBNL 47382
2. Ellis, L. B., Joubert, P. N. (1974). Turbulent Shear Flow in a Curved Duct. *Journal of Fluid Mechanics*, 62 (1), 65-84
3. Crawford, N. M., Cunningham, G., Spedding, P. L. (2003). Prediction of Pressure Drop for Turbulent Fluid Flow in 90° Bends. *Proceedings of the Institute of Mechanical Engineers*, 217(3), 153-155
4. Spedding, P. L., Benard, E., McNally, G. M. (2004). Fluid Flow through 90° Bends. *Development in Chemical Engineering and Material Processing*, 12(1-2), 107-128
5. Quamrul, H. M. (2012). CFDs Analysis of Single and Multiple Flow Characteristics in Elbow. *Engineering*, 4(4), 210-214
6. Briley, W. R., Buggeln, R. C., Donald, M. (1982). Computational of Laminar and Turbulent Flow in 90° Square Duct and Pipe Bends Using the Navier-Stokes Equation. DTIC Report No. R82-920009-F
7. Azzi, A., Friedel, L. (2005). Two upward Flow 90° Bend Pressure Loss Model. *ForschungimIngenieurwesen*, 69(2), 120-130
8. Janna, W. (1993). *Introduction to fluid Mechanics*. 3rd Edition. Boston. PWS Publishing Company
9. Blazek, J. (2005). *Computational Fluid Dynamics: Principles and Applications*, 2nd Edition, Elsevier Science, ISBN: 9780080445069
10. Ekambara, K., Mahesh, T., Dhotre, T., Jyeshtharaj, B. J. (2005). CFDs simulations of bubble column reactors: 1D, 2D and 3D approach. *Chemical Engineering Science*, 60(23), 6733-6746
11. Tomasi, N., White, R., Joseph, T. (n.d). Reservoir CFDs Modelling-What Are the Benefits of Using A 3d Model?